Metabolic Engineering 23 (2014) 145–153

Contents lists available at ScienceDirect

Metabolic Engineering

journal homepage: www.elsevier.com/locate/ymben

# Elucidation and *in planta* reconstitution of the parthenolide biosynthetic pathway

Qing Liu [a], David Manzano [b,c], Nikola Tanić [d], Milica Pesic [d], Jasna Bankovic [d], Irini Pateraki [c,e], Lea Ricard [a], Albert Ferrer [b,c], Ric de Vos [f,g,h], Sander van de Krol [a], Harro Bouwmeester [a,*]

[a] Laboratory of Plant Physiology, Wageningen University, Wageningen, The Netherlands
[b] Department of Molecular Genetics, Centre for Research in Agricultural Genomics (CRAG), CSIC-IRTA-UAB-UB, Campus UAB Bellaterra, E-08193 Barcelona, Spain
[c] Department of Biochemistry and Molecular Biology, Faculty of Pharmacy, University of Barcelona, 08028 Barcelona, Spain
[d] Department of Neurobiology, Institute for Biological Research "Sinisa Stankovic", University of Belgrade, Serbia
[e] Department of Plant and Environmental Sciences, Faculty of Science, University of Copenhagen, Thorvaldsensvej 40, Frederiksberg C, Copenhagen, Denmark
[f] Plant Research International, Wageningen, The Netherlands
[g] Centre for BioSystems Genomics, Wageningen, The Netherlands
[h] Netherlands Metabolomics Centre, Leiden, The Netherlands

ARTICLE INFO

*Article history:*
Received 27 September 2013
Received in revised form
4 March 2014
Accepted 25 March 2014
Available online 3 April 2014

*Keywords:*
Parthenolide
Biosynthetic pathway reconstitution
Feverfew
Metabolic engineering

ABSTRACT

Parthenolide, the main bioactive compound of the medicinal plant feverfew (*Tanacetum parthenium*), is a promising anti-cancer drug. However, the biosynthetic pathway of parthenolide has not been elucidated yet. Here we report on the isolation and characterization of all the genes from feverfew that are required for the biosynthesis of parthenolide, using a combination of 454 sequencing of a feverfew glandular trichome cDNA library, co-expression analysis and metabolomics. When parthenolide biosynthesis was reconstituted by transient co-expression of all pathway genes in *Nicotiana benthamiana*, up to 1.4 μg $g^{-1}$ parthenolide was produced, mostly present as cysteine and glutathione conjugates. These relatively polar conjugates were highly active against colon cancer cells, with only slightly lower activity than free parthenolide. In addition to these biosynthetic genes, another gene encoding a costunolide and parthenolide 3β-hydroxylase was identified opening up further options to improve the water solubility of parthenolide and therefore its potential as a drug.



## 1. Introduction

Sesquiterpene lactones are a major class of plant secondary metabolites and over 4000 different structures have been elucidated (Kreuger et al., 2012). Many of these colourless, frequently bitter tasting, semi-polar molecules are the bioactive constituents of a variety of medicinal plants used in (traditional) medicine (Rodriguez et al., 1976; Zhang et al., 2005). Feverfew (*Tanacetum parthenium*) is one of the most prominent medicinal species in the Asteraceae family and a well-known remedy for the treatment of various diseases (Bedoya et al., 2008). It has been used for at least two millennia for the treatment of fever, as well as headache, menstrual irregularities, stomach-ache and to relieve arthritis and inflammation (Pareek et al., 2011). Parthenolide is the principal bioactive sesquiterpene lactone component in feverfew (Bork et al., 1997). The nucleophilic nature of the methylene-γ-lactone ring and epoxide group of parthenolide enables rapid interactions with different biological targets (Mathema et al., 2012). For instance, parthenolide can promote apoptosis by inhibiting the activity of the NF-κB transcription factor complex, and thereby down-regulating anti-apoptotic genes under NF-κB control (Bork et al., 1997; Kishida et al., 2007; Parada-Turska et al., 2007; Wen et al., 2002; Zhang et al., 2009). Parthenolide has been reported to selectively target human leukaemia stem cells, while sparing normal stem or progenitor cells (Guzman et al., 2005). Despite these promising activities, application of this potent natural product is limited by its poor water-solubility (Sweeney et al., 2005). A number of chemically synthesized parthenolide derivatives with increased water solubility –hence allowing oral application - have been shown to retain bioactivity (Guzman et al., 2007; Neelakantan et al., 2009). Very recently, parthenolide and its cyclopropyl analogue have been synthesized chemically from costunolide (Long et al., 2013).

* Corresponding author.
*E-mail address:* harro.bouwmeester@wur.nl (H. Bouwmeester).

http://dx.doi.org/10.1016/j.ymben.2014.03.005
1096-7176/

Parthenolide, a germacranolide type sesquiterpene lactone, is presumably derived from costunolide, in line with the proposed precursor role of costunolide for germacranolide-, eudesmanolide- and guaianolide-type sesquiterpene lactones (de Kraker et al., 2002). The initial committed step towards the formation of costunolide is the formation of germacrene A from farnesyl diphosphate (FDP), catalysed by the enzyme (+)-germacrene A synthase (GAS) (de Kraker et al., 1998) (Fig. S1). Genes encoding GAS have been cloned from chicory (*Cichorium intybus*) (Bouwmeester et al., 2002), lettuce (*Lactuca sativa*) (Bennett et al., 2002), artemisia (*Artemisia annua*) (Bertea et al., 2006) and feverfew (Liu et al., 2011). In a number of oxidation steps, germacrene A is subsequently converted into germacra-1(10),4,11(13)-trien-12-oic acid by a cytochrome P450 enzyme, germacrene A oxidase (GAO) (de Kraker et al., 2001). Genes encoding GAO have previously been isolated from several Asteraceae species (Cankar et al., 2011; Nguyen et al., 2010). Germacra-1(10),4,11(13)-trien-12-oic acid is subsequently oxidised by costunolide synthase (COS) to 6α-hydroxy-germacra-1(10),4,11(13)-trien-12-oic acid, which undergoes spontaneous lactone ring formation to yield costunolide (de Kraker et al., 2002; Ikezawa et al., 2011; Liu et al., 2011). Finally, presumably a P450 monooxygenase catalyses the epoxidation of the C4-C5 double bond of costunolide, yielding parthenolide (Liu et al., 2011). The gene encoding the enzyme responsible for that epoxidation, *parthenolide synthase* (*PTS*), has not been reported yet.

Elucidation of all parthenolide biosynthetic pathway and cloning of the structural genes may enable the production of parthenolide in heterologous systems. Therefore, we set out to identify and isolate all the genes of the parthenolide biosynthetic pathway in feverfew. We have previously reported on the *TpGAS* gene from feverfew (Majdi et al., 2011). Here we report on the isolation and characterisation of the remaining genes required for parthenolide biosynthesis in feverfew (*TpGAO*, *TpCOS* and *TpPTS*). Enzyme activities were characterized by expression of genes in yeast and subsequently the complete parthenolide biosynthetic pathway was reconstituted in *Nicotiana benthamiana,* by co-expression of *TpGAS* with the newly identified *TpGAO*, *TpCOS* and *TpPTS*. Extracts of *N. benthamiana* leaves co-expressing these genes contained free parthenolide, as well as cysteine and glutathione (GSH) conjugates of parthenolide. Because the conjugation to cysteine and GSH affects water solubility, we assessed the biological activity of these parthenolide derivatives in cancer cell lines. The parthenolide conjugates were less effective than free parthenolide but still displayed considerable anti-cancer activity, particularly in colon cancer cells. In addition to the parthenolide biosynthetic genes, another candidate gene was identified to encode a 3β-hydroxylase that uses costunolide as well as parthenolide as substrate. This may give additional possibilities to improve the water solubility of parthenolide. The production of parthenolide and more water-soluble conjugates through metabolic engineering of heterologous hosts may provide a sustainable alternative source for the further development of parthenolide as an anti-cancer drug.

## 2. Materials and methods

Detailed description of the Gene expression analysis, Headspace analysis and Thermodesorption GC–MS, LC-QTOF-MS LC-Orbitrap-FTMS analysis of leaf extracts, parthenolide detection and quantification by LC-MRM-MS and Cysteine and glutathione (GSH) conjugation can be found in the supplementary data.

### 2.1. Isolation and cloning of full length candidate genes from feverfew

An EST library constructed from mRNA isolated from feverfew (*Tanacetum parthenium*) trichomes as reported before (Majdi et al., 2011) was used for gene isolation. For *TpGAO* and *TpCOS* candidates, one contig was identified for each gene by sequence homology to known GAOs (*LsGAO*, GU198171; *CiGAO*, GU256644; *SlGAO*, GU256646; *HaGAO*, GU256645; *BsGAO*, GU256647) and COSs (*LsCOS*, AEI59780; and *CiCOS*, AEG79727) (Fig. S2). Twenty-eight parthenolide synthase candidate cytochrome P450 contigs were identified by sequence homology to known sesquiterpene monooxygenases of the CYP71 subfamily. Four of them, *Tp2116*, *Tp4149*, *Tp9025* and *Tp8878*, were selected for functional characterization based on their expression profile during ovary development. RACE PCR (Clontech) was used to obtain the sequence of the 5′- and 3′-region of all candidate contigs. Full length cDNAs of candidate genes were amplified from feverfew cDNA with the addition of *NotI*/*PacI* restriction sites. The cDNAs were subsequently cloned into the yeast expression vector pYEDP60 (Pompon et al., 1996) and sequenced. The cDNA sequences of all candidates genes have been deposited in GenBank: *TpGAO*, KC964544; *TpCOS*, KC964545, *Tp8878*, KC954153; *Tp9025*, KC954154; *Tp2116* (*TpPTS*), KC954155; *Tp4149*, KC954156. The sequences were also submitted to David Nelson's cytochrome P450 homepage (http://drnelson.uthsc.edu/cytochromeP450.html), *Tp2116* and *Tp8878* were assigned the name as CYP71CA1 and CYP71CB1, respectively (Nelson, 2009).

### 2.2. Plasmid construction for gene expression in yeast

*TpGAO, TpCOS* and three parthenolide synthase candidates (*Tp2116*, *Tp4149*, *Tp9025*) were cloned into pYED60 vector using *NotI*/*PacI* restriction sites. The obtained constructs were named *TpGAO::pYED60, TpCOS::pYED60*, *Tp2116::pYED60*, *Tp4149::pYED60*, and *Tp9025::pYED60. TpGAS::pYES3*(Liu et al., 2011) plus *TpGAO::pYED60* and *TpGAS*/*TpGAO::pESC-Trp* plus *TpCOS::pYEDP60* were co-transformed into the WAT11 (Urban et al., 1997) yeast strain. After transformation yeast clones containing both plasmids were selected on SD minimal medium supplemented with amino acids, but omitting uracil, adenine sulphate and L-tryptophane for auxotrophic selection of transformants.

### 2.3. Yeast in vitro microsome assay

The procedure of the yeast microsome isolation is described in detail in the supplementary data. For *in vitro* microsome assays, 72 µl isolated microsomal fractions, 10 µl substrate (of a 10 mM stock in DMSO), 100 µl NADPH (of a 10 mM stock in 100 mM potassium buffer), 20 µl potassium buffer (1 M, pH7.5), and 288 µl water were mixed and incubated for 2.5 h at 25 °C with shaking (200 rpm). Then the mixture was centrifuged at 12,000 rpm for 10 min. The supernatant was filtered through an 0.22 µm filter before analysis of the products by LC-Orbitrap-FTMS (for details see supplementary data).

### 2.4. Plasmid construction and transient expression in Nicotiana benthamiana

For transient expression in *N. benthamiana*, *TpGAS*, *TpGAO*, *TpCOS*, *Tp8878*, and three parthenolide synthase candidates (*Tp2116*, *Tp4149*, *Tp9025*) were cloned into ImpactVector1.1 (http://www.wageningenur.nl/en/show/Productie-van-farmaceutische-en-industriele-eiwitten-door-planten.htm) to express them under the control of the Rubisco (RBC) promoter (Outchkourov et al., 2003). *TpGAS* was also cloned into ImpactVector1.5 to fuse it with the RBC promoter and the CoxIV mitochondrial targeting sequence as we have demonstrated before that mitochondrial targeting of sesquiterpene synthases results in improved sesquiterpene production (2011). An LR reaction (Gateway-LR Clonase TM II) was carried out to clone each gene into the pBinPlus binary vector (Vanengelen et al., 1995) between the right and left borders of the T-DNA for plant transformation. *A. tumefaciens* infiltration

(agro-infiltration) for transient expression in *N. benthamiana* was performed as described by Liu et al. (2011). After infiltration the plants were grown for another four and half days and then harvested for analysis.

## 3. Results

### 3.1. Identification of parthenolide biosynthesis candidate genes

Previously we have shown that parthenolide accumulates to high levels in floral glandular trichomes of feverfew (*Tanacetum parthenium*) (Majdi et al., 2011). To identify the genes involved in this parthenolide biosynthesis, mRNA was extracted from isolated flower trichomes and used for deep-sequencing to obtain a feverfew trichome EST database (Majdi et al., 2011). Subsequently, sequences of reported Asteraceae *GAO*s and *COS*s were used to blast against the feverfew EST database. Two sets of EST sequences with the highest homology to chicory *GAO* and chicory *COS* were assemble into two contigs from which full length open reading frames (ORF) were obtained. The expression of *TpGAS*, putative *TpGAO*, and putative *TpCOS* was profiled in feverfew during ovary development with real time RT-PCR. Those three genes showed similar patterns of expression, which was highest in stage 2 and stage 3 ovaries, and then decreased from stage 4 untill virtually zero in stage 6 (Fig. 1B). Moreover, the expression pattern of *TpGAS*, the putative *TpGAO*, and the putative *TpCOS* is consistent with the accumulation profile of parthenolide in ovaries during flower development (Fig. 1): the parthenolide content increased from stage 2 to stage 5, and then decreased slightly. The content of its precusor, costunolide, increased in stage 2 and 3 and then decreased.

Most sesquiterpene-modifying P450s belong to the CYP71 subfamily (Ikezawa et al., 2011). Indeed, the putative feverfew *TpGAO* and *TpCOS* belong to this CYP71 subfamily. Identification of the expected parthenolide synthase (*TpPTS*) gene therefore was focussed on P450 sequences showing closest homology to the CYP71 class. Screening of the feverfew EST sequence database for putative *TpPTS* candidates identified 28 P450 contigs that belong to the CYP71 family and all have relatively high amino acid sequence similarity with *TpCOS*. To limit the number of candidate genes to be characterized for enzymatic activity, we compared the expression profiles of the candidate genes with *TpGAS*, and the putative *TpGAO* and *TpCOS*, assuming that *TpPTS* will have a similar expression pattern as the upstream genes. Three out of the 28 candidate genes – *Tp2116*, *Tp4149*, and *Tp9025* – showed maximum expression in ovary development stage 2–4, similar as *TpGAS*, putative *TpGAO* and *TpCOS* and were therefore considered as *TpPTS* candidate genes (Fig. 1D). Costunolide and parthenolide levels decreased slighly after stage 4 (Fig. 1A), which suggests further metabolism of costunolide and parthenolide in these late stages. Indeed, one of the candidate genes (*Tp8878*) displayed increased expression after ovary development stage 4 (Fig. 1D) and was therefore considered as pathway-side branch candidate gene for

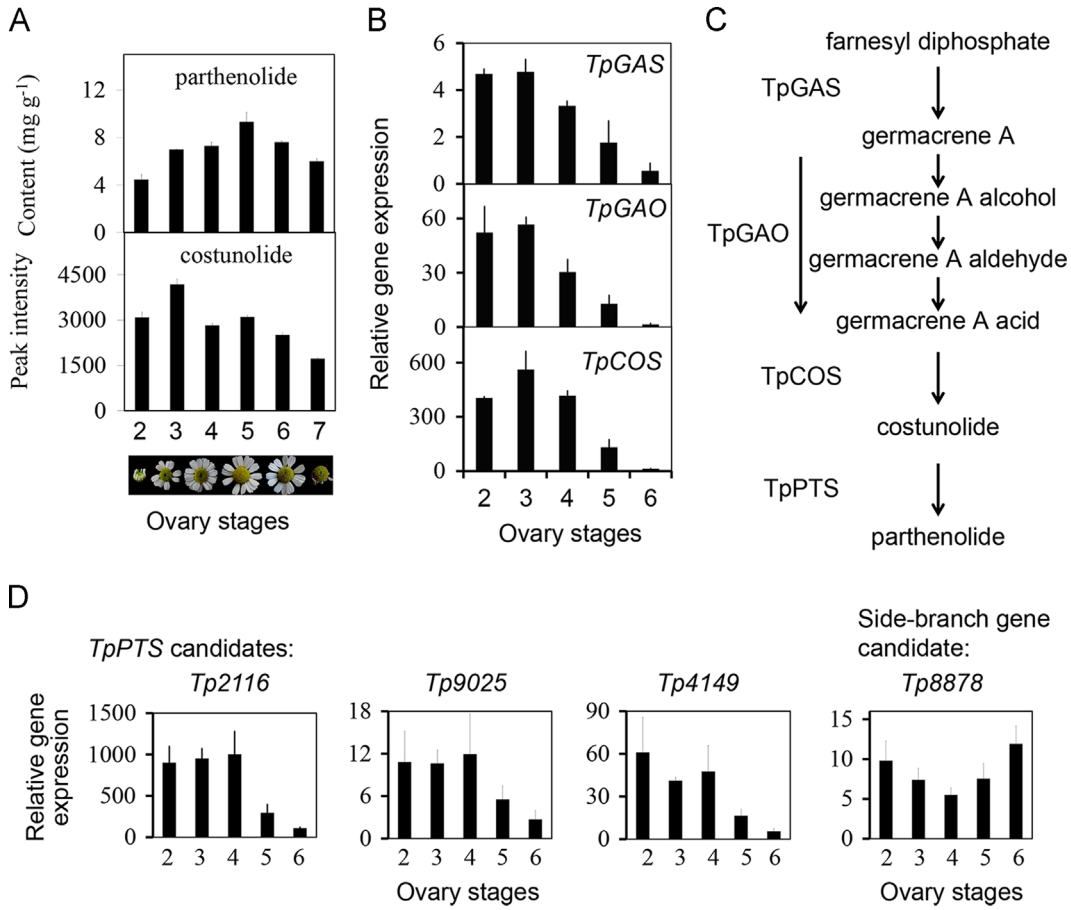


**Fig. 1.** Parthenolide and costunolide content, and expression profile of parthenolide synthase candidates genes during ovary development. (A) Costunolide and parthenolide content in different developmental stages of feverfew ovaries. Bars represent means ($n=3$) ± S.E. (B) Gene expression profile of feverfew *germacrene A synthase* (*TpGAS*), *germacrene A oxidase* (*TpGAO*), and *costunolide synhtase* (*TpCOS*) during ovary development. (C) Simplified biosynthetic pathway of parthenolide in feverfew. (D) Gene expression profile of *parthenolide synthase* (*TpPTS*) candidates and single-branch gene candidate during ovary development.

costunolide and/or parthenolide conversion. The ORFs of putative *TpGAO* and *TpCOS*, three *TpPTS* candidates (*Tp2116*, *Tp4149*, *Tp9025*), and one pathway side branch candiate (*Tp8878*) were cloned into yeast expression vector pYED60 for expression and characterization.

### 3.2. Functional characterization of parthenolide biosynthesis genes in yeast

#### 3.2.1. TpGAO and TpCOS candidates

To test the enzymatic function of the putative *TpGAO*, this gene was expressed in yeast together with the previously characterized gene *TpGAS* (Majdi et al., 2011), and crude yeast extracts were subsequently prepared and analyzed by GC–MS for the presence of sesquiterpene lactones. Cells expressing *TpGAS*+*TpGAO* showed a clear GC–MS peak of elementrien-12-oic acid, which is missing in cells expressing *TpGAS* alone. This compound is a cope-rearrangement product of germacra-1(10),4,11(13)-trien-12-oic acid (Fig. S3), showing that the protein encoded by *TpGAO* is able to catalyze oxidation of germacrene A to germacra-1(10),4,11(13)-trien-12-oic acid. To test the catalytic function of the putative *TpCOS*, the gene was co-expressed with *TpGAS* and *TpGAO* in yeast. Compared to the products produced by yeast cells expressing both *TpGAS* and *CiGAO*, the extracts of yeast cells expressing *TpGAS*+*TpGAO*+*TpCOS* showed a new GC–MS peak which was identified as costunolide, while the peak for germacra-1(10),4,11(13)-trien-12-oic acid was strongly reduced (Fig. S3). Thus, it is confirmed that the protein encoded by the putative *TpCOS* gene is able to catalyze the conversion of germacra-1(10),4,11(13)-trien-12-oic acid to costunolide.

#### 3.2.2. Characterization of parthenolide synthase candidates

To test the catalytic activity of *TpPTS* candidates, microsomes of yeast expressing *Tp2116*, *Tp4149*, and *Tp9025* were isolated and incubated with costunolide. Compared to the microsomes from yeast transformed with the control consturct, the microsomes from yeast expressing *Tp2116* induced a new LC-MS peak that was unambigously identified as parthenolide ($[M+H]^+=249$, retention time and mass spectrum match with that of the parthenolide standard) (Fig. 2). An official name CYP71CA1 was assigned to this parthenolide synhtase (*TpPTS*). No new peaks were detected in the assays with microsomes isolated from yeast expressing *Tp4149* or *Tp9025*.

To test the catalytic activity of *Tp8878*, a candidate assumed to be involved in a side branch of parthenolide biosynthesis, microsomes of yeast transformed with *Tp8878* were isolated and incubated with costunolide or parthenolide. With parthenolide as a substrate, a new LC-MS peak was detected which was identified as 3β-hydroxyparthenolide ($[M+H]^+=265$, retention time and mass spectrum matches that of the 3β-hydroxyparthenolide standard) (Fig. 3A and B). With costunolide as a substrate, also a new product peak was detected, which was identified as 3β-hydroxycostunolide ($[M+H]^+=249$, retention time and mass spectrum matches that of a 3β-hydroxycostunolide standard) (Fig. 3C and D). An official name CYP71CB1 was assigned to this 3β-hydroxylase.

### 3.3. Reconstitution of the parthenolide biosynthetic pathway in Nicotiana benthamiana

With all the genes for the production of parthenolide available, we aimed to reconstitute the parthenolide biosynthetic pathway in the plant host *N. benthamiana* through transient heterologous gene expression. In addition, we tested the effect on product accumulation of the co-expression of the pathway genes together with a soluble *Arabidopsis thaliana* HMG-CoA reductase (*AtHMGR*) which can increase FDP substrate availibity needed for the pathway. Hereto, the *AtHMGR*, *TpGAS*, *TpGAO*, *TpCOS* and *TpPTS* (*CYP71CA1*) coding sequences were cloned into the binary expression vector pBIN under the control of the Rubisco promoter (RBC). *Agrobacterium tumefaciens* was transformed with the various binary expression vectors and leaves were co-infiltrated with different combinations of the transformed *A. tumefaciens* strains to reconstitute the parthenolide biosynthetic pathway in *N. benthamiana* step by step.

#### 3.3.1. TpGAS and TpGAS+TpGAO

Four days after infiltration with the *A. tumefaciens* strain carrying the RBC:TpGAS construct, the *N. benthamiana* leaves emitted the volatile compound germacrene A into their headspace (Table 1 and Fig. S4). When leaves were co-infiltrated with two *A. tumefaciens* strains carrying the *TpGAS* and *TpGAO* constructs, respectively, germacrene A levels in the headspace were reduced by 90% compared to infiltration with *TpGAS* alone, suggesting that *Tp*GAO can efficiently utilise germacrene A. However, no new product peaks were detected neither in the headspace nor in dichloromethane (DCM) extracts of the infiltrated leaves, indicating that the expected

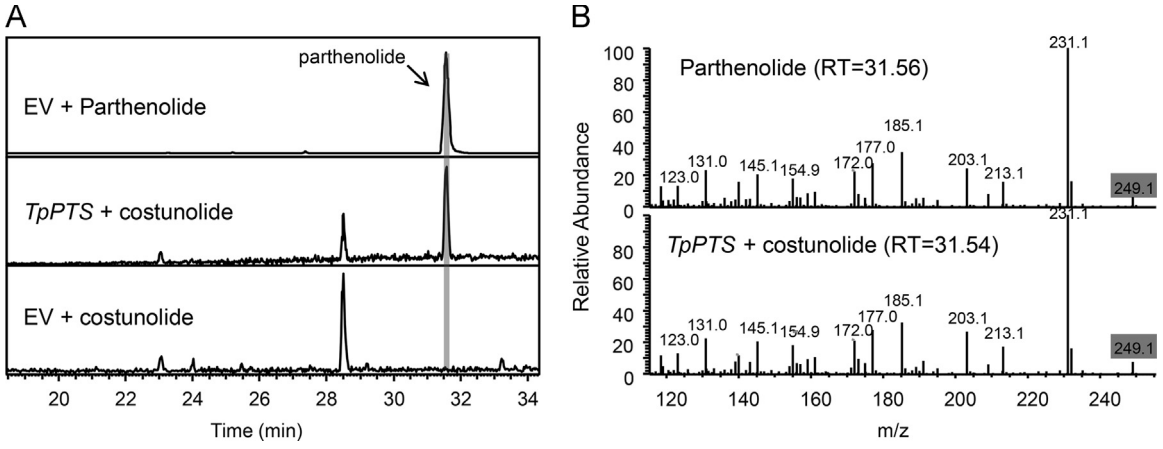


**Fig. 2.** Identification of *Parthenolide Synthase* (*TpPTS*) using a yeast microsome assay. (A) LC-Orbitrap-FTMS (liquid chromatography-orbitrap-fourier transform mass spectrometry) chromatogram at $m/z=249.14852$ (10 ppm, positive ionization mode) analysis of yeast microsome assays. EV (empty vector)+parthenolide: microsome of yeast expressing empty vector fed with parthenolide; *TpPTS*+costunolide: microsome of yeast expressing *TpPTS* fed with costunolide; EV+costunolide: microsome of yeast expressing empty vector fed with costunolide. Peaks with identical retention time and mass are indicated by grey bar. (B) The fragmentation patterns of the peaks marked by the grey bar in Fig. 2A (retention times are also given): parthenolide standard and the microsome assay *TpPTS*+costunolide. Grey boxes indicate the parent ion at $[M+H]^+=249.14852$.

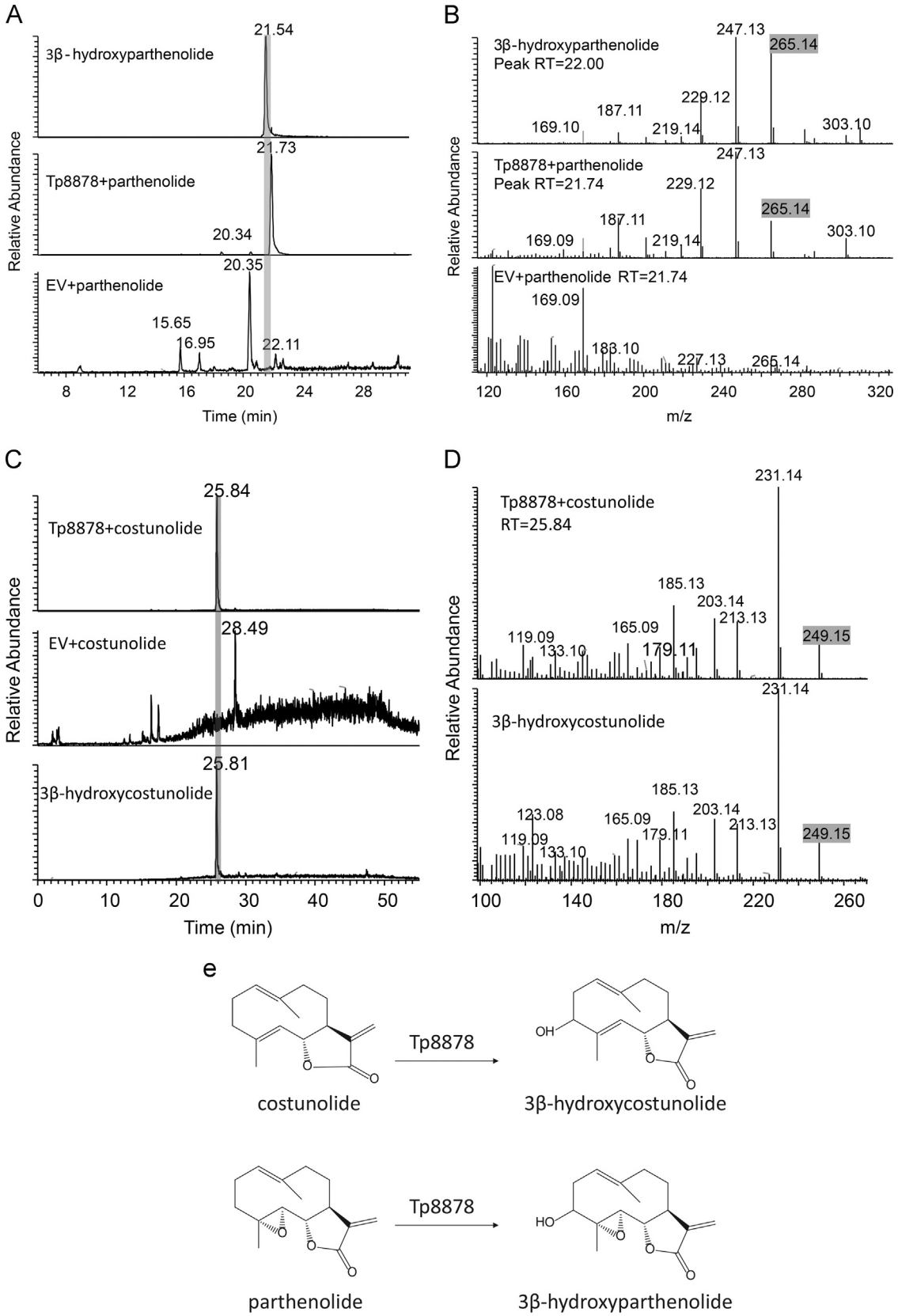


**Fig. 3.** Functional Identification of *Tp8878* Using a Yeast Microsome Assay. (A) LC-Orbitrap-FTMS chromatogram at $m/z=265.14344$ (10 ppm, positive ionization mode) analysis of yeast microsome assays. Tp8878+parthenolide: microsome of yeast expressing *Tp8878* fed with parthenolide; EV+parthenolide: microsome of yeast expressing empty vector fed with parthenolide. Peaks with identical retention time and mass are indicated by grey bar. (B) The fragmentation patterns of the peaks marked by the grey bar in Fig. 3A (retention times are also given): 3β-hydroxyparthenolide standard and the microsome assay *Tp8878*+parthenolide. Grey boxes indicate the parent ion at $[M+H]^+=265.14344$. (C) LC-Orbitrap-FTMS chromatogram at $m/z=249.14852$ (10 ppm, positive ionization mode) analysis of yeast microsome assays. Tp8878+costunolide: microsome of yeast expressing *Tp8878* fed with costunolide; EV+costunolide: microsome of yeast expressing empty vector fed with costunolide. Peaks with identical retention time and mass are indicated by grey bar. (D) The fragmentation patterns of the peaks marked by the grey bar in Fig. 3C (retention times are also given): 3β-hydroxycostunolide standard and the microsome assay *Tp8878*+costunolide. Grey boxes indicate the parent ion at $[M+H]^+=249.14852$. (E) Molecular structures of costunolide, 3β-hydroxycostunolide, parthenolide, and 3β-hydroxyparthenolide.

**Table 1**
New metabolites detected in *N. benthamiana* leaves agro-infiltrated by different combinations of genes.

| Metabolites | Combinations of genes transiently expressed in *N. benthamiana* leaves[a] | | | | | |
|---|---|---|---|---|---|---|
| | ***GAS*** | ***GAS*+*GAO*** | ***GAS*+*GAO*+*COS*** | ***GAS*+*GAO*+ *COS*+ *PTS*** | ***AtHMGR*+ *GAS*+*GAO*+*COS*+ *PTS*** | ***AtHMGR*+ *GAS*+*GAO*+ *COS*+ *PTS*+*8878*** |
| Germacrene A | ††[b] | † | –[c] | – | – | – |
| Germacra-1(10),4,11(13)-trien-12-oic acid | – | – | – | – | – | – |
| Costunolide | – | – | †† | † | †† | †† |
| Costunolide-GSH | – | – | ††† | †† | ††† | ††† |
| Costunolide-cysteine | – | – | †††† | ††† | †††† | †††† |
| Parthenolide | – | – | – | – | † | † |
| Parthenolide-GSH | – | – | – | † | †† | †† |
| Parthenolide-cysteine | – | – | – | †† | ††† | ††† |
| 3β-hydroxycostunolide | – | – | – | – | – | – |
| 3β-hydroxycostunolide-GSH | – | – | – | – | – | † |
| 3β-hydroxycostunolide-cysteine | – | – | – | – | – | †† |
| 3β-hydroxyparthenolide | – | – | – | – | – | – |
| 3β-hydroxyparthenolide-GSH | – | – | – | – | – | – |
| 3β-hydroxyparthenolide-cysteine | – | – | – | – | – | – |

[a] GAS, germacrene A synthase; GAO, germacrene A oxidase; COS, costunolide synthase; PTS, parthenolide synthase; 8878, 3β-hydroxylase.
[b] †: Metabolites detected by LC-MS. The number of † indicates their relative level.
[c] Means metabolites not detected by LC-MS.

products of the *Tp*GAO enzyme, germacra-1(10),4,11(13)-trien-12-ol, germacra-1(10),4,11(13)-trien-12-al and germacra-1(10),4,11(13)-trien-12-oic acid, are not stable *in planta* or are further metabolized into other products, analogous to our previous results obtained with the heterologous expressed *CiGAO* gene (Liu et al., 2011). Using high mass resolution LC-QTOF-MS in negative ionization mode, we checked whether any germacra-1(10),4,11(13)-trien-12-oic acid produced was possibly glycosylated within the *N. benthamiana* leaves, but accurate mass signals corresponding to the elemental formulae of the acid conjugated to either a hexose, a deoxyhexose or a pentose, or to combinations thereof, were not detected. We nevertheless decided to infiltrate the next gene of the pathway to see if the anticipated product and hence the substrate of the next enzyme was produced or not.

### 3.3.2. *TpGAS* +*TpGAO*+*TpCOS*

Co-infiltration of *A. tumefaciens* strains carrying the *TpGAS*, *TpGAO* and *TpCOS* expression constructs did result in the production of costunolide at 4 days post-infiltration (Table 1 and Fig. S5A). The average production of costunolide was $9.6 \pm 0.8$ μg $g^{-1}$ FW ($n=8$). No costunolide was detected in extracts from leaves upon transient expression of the empty vector (pBIN), neither in those of *TpGAS* alone, *TpGAS*+*TpGAO* or *TpGAS*+*TpCOS*, indicating that the production of costunolide in *N. benthamiana* leaves is dependent on the presence of three genes: *TpGAS*, *TpGAO* and *TpCOS*.

To investigate whether there were any other unexpected products formed in the infiltrated leaves, we performed untargeted LC-QTOF-MS analysis of leaf extracts. This resulted in the detection of two chromatographic peaks eluting at 22.24 and 22.48 min in leaves infiltrated with *TpGAS*+*TpGAO*+*TpCOS* that were absent in leaves infiltrated with *TpGAS*+*TpGAO* (Fig. S5B-E). These two *Tp*COS-induced products were identified as the cysteine and glutathione (GSH) conjugates of costunolide, respectively.

### 3.3.3. *TpGAS* +*TpGAO*+*TpCOS*+*TpPTS with boosting by AtHMGR*

No free parthenolide was detected in leaf extracts transiently expressing the four genes *TpGAS*+*TpGAO*+*TpCOS*+*TpPTS* (Table 1). In an attempt to boost the availability of substrate for the parthenolide pathway, we also co-expressed *AtHMGR*. In combination with *TpGAS*+*TpGAO*+*TpCOS*, this resulted in 4-fold increased costunolide production (Fig. S6B). When *AtHMGR* was co-expressed with *TpGAS*+*TpGAO*+*TpCOS*+*TpPTS*, free parthenolide was detected (2.05 ng $g^{-1}$ FW) 4 days after infiltration by MRM-LC-MS (Fig. S6A). Moreover, two new LC-QTOF-MS peaks eluting at 17.74 and 18.53 min were detected, which were absent in leaves infiltrated with *TpGAS*+*TpGAO*+*TpCOS*+*pBIN* as control. The exact mass and comparison with standards identified these products as the cysteine and GSH conjugates of parthenolide (Fig. S6C-F).

### 3.3.4. *TpGAS* +*TpGAO*+*TpCOS*+*TpTPS*+*Tp8878 with boosting by AtHMGR*

To verify the function of *Tp8878* (*CYP71CB1*) *in planta*, *A. tumefaciens* strains with the parthenolide pathway constructs plus *AtHMGR* were infiltrated into *N. benthamiana* together with *A. tumefaciens* with the *Tp8878* expression construct. Compared with the control (parthenolide pathway without *Tp8878*) one new peak (RT = 14.68 min) was detected that was identified as 3β-hydroxycostunolide-GSH (both retention time and mass spectrum match that of a 3β-hydroxycostunolide-GSH standard) (Table 1 and Fig. S7A-B). A second new peak was identified as 3β-hydroxycostunolide-cysteine. GSH or cysteine conjugates of 3β-hydroxyparthenolide was not detectable in these samples. Compared with leaves infiltrated with only the costunolide pathway, about 50% of the original costunolide conjugates were converted into parthenolide when *TpPTS* was added to the infiltration mix. When *Tp8878* was co-infiltrated with the costunolide pathway together with *TpPTS*, about 40% of the costunolide conjugates were converted. Yet the amount of parthenolide conjugates was decreased by 71% compared to that of leaves infiltrated with the costunolide pathway plus *TpPTS* (Fig. S7C). This is possibly the result of 3-hydroxylation of parthenolide by *Tp8878*, as we showed to occur in yeast microsomes (Fig. 3), but we were unable to detect any parthenolide-derived compounds.

### 3.4. Anti-cancer activity of parthenolide conjugates in cell lines

The anti-cancer effect of parthenolide GSH and cysteine conjugates was examined in eight different human cell lines: both sensitive and multi-drug resistant lines of non-small cell lung carcinoma, glioblastoma and colon carcinoma cells as well as normal human keratinocytes (Table 2). Parthenolide-cysteine and parthenolide-GSH conjugates were less potent than free parthenolide: the

**Table 2**
IC 50 values (μM) of parthenolide and its conjugates acquired by sulforhodamine B viability test.

| Compounds | NCI-H460[a] | NCI-H460/R[b] | U87[c] | U87-TxR[d] | DLD1[e] | DLD1-TxR[f] | HT-29[e] | HaCaT[g] |
|---|---|---|---|---|---|---|---|---|
| Parthenolide | **2.1** | **6.8** | **40.5** | **26.7** | **2.1** | **1.8** | **3.6** | **10.6** |
| Parthenolide-Cysteine | **76.8** | **46.9** | **107.7** | **105.0** | **37.0** | **33.1** | **17.3** | **65.7** |
| Parthenolide-Glutathione | **71.4** | **44.7** | **120.8** | **83.3** | **29.2** | **23.1** | **10.7** | **57.9** |

[a] Sensitive non-small cell lung carcinoma cell line.
[b] Multi-drug resistant non-small cell lung carcinoma cell line derived from its sensitive counterpart.
[c] Sensitive glioblastoma cell line.
[d] Multi-drug resistant glioblastoma cell line derived from its sensitive counterpart.
[e] Sensitive colon carcinoma cell lines.
[f] Multi-drug resistant colon carcinoma cell line derived from its sensitive counterpart DLD1.
[g] Normal human keratinocyte.

concentrations necessary to inhibit cell growth by 50% (IC50 values) for conjugates were significantly higher than for free parthenolide in all tested cancer cell lines and normal human keratinocytes. Nevertheless, IC50 values of the conjugates for colon cancer cells are substantially lower than those for normal cells (HaCaT), indicating selectivity of both parthenolide conjugates towards colon carcinoma cells. The parthenolide-cysteine and parthenolide-GSH conjugates exerted the highest bioactivity in HT-29 cells (colon adenocarcinoma) with IC50s of 17.3 and 10.7 μM, respectively. The sensitivity to free or conjugated parthenolide was not affected by multi-drug resistance as the inhibitory profiles of the compounds were similar in both sensitive (DLD1) and resistant (DLD1-TxR) colon carcinoma cell lines (Table 2, Fig. S8). Cysteine and GSH, when applied alone, had no influence on cell growth (Fig. S8).

## 4. Discussion

The sesquiterpene lactone parthenolide from feverfew is a promising anti-cancer drug. The identification of feverfew *parthenolide synthase* (*TpPTS*) which uses costunolide as substrate confirms the hypothesis that parthenolide is derived from costunolide through epoxidation of the C4-C5 double bond (Liu et al., 2011). With the identified *germacrene A synthase* (*TpGAS*) (Majdi et al., 2011), *germacrene A oxidase* (*TpGAO*), *costunolide synthase* (*TpCOS*) and *TpPTS* we have isolated all structural genes of the biosynthetic pathway from the universal sesquiterpene precursor farnesyl diphosphate (FDP) (Majdi et al., 2011) up to parthenolide. Expression of these genes in the heterologous hosts *Nicotiana benthamiana* results in the formation of parthenolide plus a number of parthenolide conjugates, which may provide an attractive option for a more efficient and controlled production of this compound. The successful identification of the *TpPTS* gene shows that gene mining based on sequence similarity to related enzymes in combination with gene expression profiling is a good strategy to identify candidate genes involved in plant secondary metabolite pathways.

In the present study we showed that the production of parthenolide in a heterologous host plant species is feasible. No free parthenolide was detected in *N. benthamiana* leaves infiltrated with *TpGAS*+*TpGAO*+*TpCOS*+*TpPTS* by sensitive UPLC-MRM-MS, but when *AtHMGR* was added to boost the supply of the precursor FDP, indeed a trace amount of free parthenolide (2.05 ng $g^{-1}$ FW) was detected. This low amount of free parthenolide was caused by the conjugation of the parthenolide produced towards both parthenolide-cysteine (1368.4 ng $g^{-1}$ FW) and parthenolide-GSH (87.5 ng $g^{-1}$ FW) conjugates. As costunolide, parthenolide and the hydroxylated products are cytotoxic, conjugation to GSH or cysteine may be part of a detoxification reaction of the *N. benthamiana* host cells. The cysteine-conjugates may be produced from the GSH-conjugate through the actions of peptidases (Marrs, 1996). As the conjugation to GSH is reversible (Heilmann et al., 2001) at physiological pH and the conjugation to cysteine is not, this would explain the relatively high levels of cysteine-conjugated products.

To increase productivity during multi-step pathway reconstitution, it is important to boost the flux through the pathway or make use of pathway precursors more efficiently (Alonso et al., 2011; Houshyani et al., 2013). As the biosynthesis of parthenolide is highly compartmentalized, like other terpenoids, enzymes need to be targeted to the appropriate location to achieve better production (Dong et al., 2013).

More than 90% of the total parthenolide produced in *N. benthamiana* was conjugated to either cysteine or GSH, while more than 95% of the parthenolide detected in the trichomes of feverfew was present as free parthenolide. *TpGAS* was found to be expressed much higher in the trichomes compared in the other tissues (Majdi et al., 2011). Trichome specific expression of a diterpene synthase in transgenic tobacco was recently reported (Ennajdaoui et al., 2010). To obtain higher production of free parthenolide in heterologous plants host, it would be a good option to try tissue specific expression in trichomes to prevent conjugation. An alternative host could be lettuce (*Lactuca sativa*) or chicory (*Cichorium intybus*). Both can produce costunolide and its derivatives that are accumulating in specialized structures called laticifers throughout the plant (Hagel et al., 2008). Thus lettuce and chicory could potentially be used as a production platform for the heterologous production of parthenolide.

As water solubility is one of the major limiting factors for parthenolide being used as an anti-cancer drug (Shanmugam et al., 2006), obtaining more water-soluble parthenolide derivatives or analogues can be of interest. We have isolated *Tp8878* and showed that it encodes a cytochrome P450 enzyme that can oxidise both costunolide and parthenolide to produce the more polar derivatives 3β-hydroxycostunolide and 3β-hydroxyparthenolide respectively (Fig. 3). Indeed, both compounds have also been detected in feverfew extracts (Fischedick et al., 2012). Hydroxylation makes these compounds more polar and may also allow additional enzymatic or chemical modifications to further improve water solubility. 3β-Hydroxyparthenolide has been shown to activate an anti-oxidant response which may be useful for the treatment of neurodegenerative disease (Fischedick et al., 2012), suggesting the additional hydroxyl group does not compromise its biological activity.

Previous studies have demonstrated the anti-cancer property of parthenolide *in vitro*, through induction of apoptotic cell death in a number of human cancer cell lines (Mathema et al., 2012). The depletion of intracellular GSH by parthenolide probably contributes to its apoptotic activity (Wen et al., 2002; Zhang et al., 2004), indicating that the anti-cancer effect of parthenolide involves interaction with GSH. Indeed, in our study, the parthenolide-GSH and parthenolide-cysteine conjugates showed less biological activity than free parthenolide in the cancer cell lines investigated. However, even though less effective in most cell lines, these conjugates showed quite high and selective activity against colon carcinoma cells and this feature could be an advantage in colon cancer treatment. Perhaps they act as a pro-drug in these cells, requiring biotransformation into free parthenolide to exert the anti-cancer effect.

The relative polarity (hydrophilicity) of the sesquiterpene lactones identified in this study can be deduced from their relative

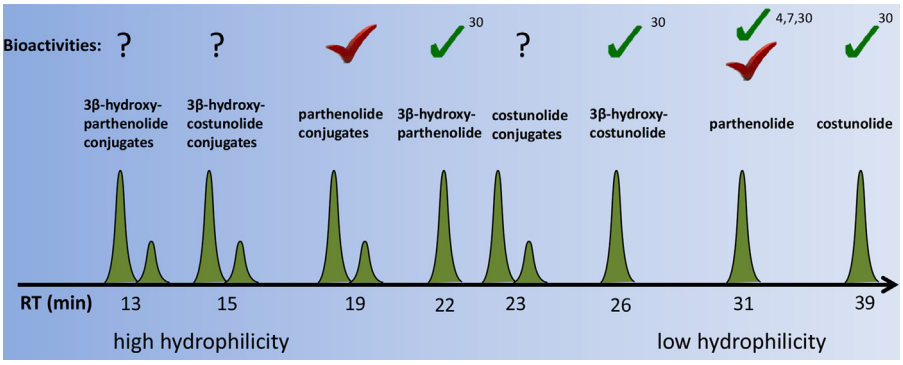


**Fig. 4.** Relative Hydrophilicity And Bioactivity of Compounds Identified During the Reconstitution of the Parthenolide Biosynthetic Pathway in *N. benthamiana*. The *x*-axis indicates the retention time of compounds using C18 reverse phase HPLC. The higher the retention time, the lower the hydrophilicity of the molecule. Green (smaller)-check marks indicate that bioactivities of the corresponding compounds have been reported; the numbers after the green-check marks indicating the corresponding references; question marks indicate that the bioactivities of corresponding compounds are unknown; red (bigger)-check mark indicates that the bioactivity of the corresponding compound has been identified in the present study. (For interpretation of the references to color in this figure caption, the reader is referred to the web version of this paper.)

retention times in the C18 reverse phase LC-MS chromatograms (Fig. 4). Considering that poor water-solubility of parthenolide (and its oxidised derivatives) is a significant limitation for its application in cancer treatment (Sweeney et al., 2005). Several parthenolide amino acid derivatives have been reported to active against some cancer cell lines (Nasim and Crooks, 2008; Song et al., 2014; Woods et al., 2011). In this study, parthenolide-conjugates are selectively active against colon cancer cells. Thus the conjugation of parthenolide and its oxidised derivatives could be a new strategic tool in drug development for cancer treatment.

In conclusion, the isolation of the genes encoding the entire parthenolide biosynthetic pathway will enable the industrial scale production of parthenolide in heterologous systems such as plants, yeast or other micro-organisms. The success of that will improve the availability of parthenolide – and parthenolide derivatives with improved chemical properties – and hence speed up the development of parthenolide-based anti-cancer drugs.

## Funding

This work was funded by the European Commission (EU-project TerpMed, Plant Terpenoids for Human Health: a chemical and genomic approach to identify and produce bioactive compounds, Grant agreement no.: 227448). Ric C.H. de Vos acknowledges additional funding by the Netherlands Metabolomics Centre and the Centre for BioSystems Genomics, both of which are part of the Netherlands Genomics Initiative/Netherlands Organization for Scientific Research. The funders had no role in study design, data collection and analysis, decision to publish, or preparation of the manuscript.

## Acknowledgements

We thank Francel Verstappen for assistance with MRM-LC-MS analysis, Bert Schipper for assistance with LC-QTOF-MS and LC-Orbitrap-MS analysis, Miriam Goedbloed for assistance with making expression constructs, Justin T. Fischedick for providing standards isolated from feverfew. This project was funded by the European Commission (EU-project TerpMed, Plant Terpenoids for Human Health: a chemical and genomic approach to identify and produce bioactive compounds, Grant agreement no.: 227448). Ric C.H. de Vos acknowledges additional funding by the Netherlands Metabolomics Centre and the Centre for BioSystems Genomics, both of which are part of the Netherlands Genomics Initiative/Netherlands Organization for Scientific Research.

## Appendix A. Supplemantary material

Supplementary data associated with this article can be found in the online version at http://dx.doi.org/10.1016/j.ymben.2014.03.005.

## References

Alonso, A.P., Val, D.L., Shachar-Hill, Y., 2011. Central metabolic fluxes in the endosperm of developing maize seeds and their implications for metabolic engineering. Metab. Eng. 13, 96–107.
Bedoya, L.M., Abad, M.J., Bermejo, P., 2008. The role of parthenolide in intracellular signalling processes: review of current knowledge. Curr. Signal Transduct. Therapy 3, 82–87.
Bennett, M.H., Mansfield, J.W., Lewis, M.J., Beale, M.H., 2002. Cloning and expression of sesquiterpene synthase genes from lettuce (*Lactuca sativa* L.). Phytochemistry 60, 255–261.
Bertea, C.M., Voster, A., Verstappen, F.W.A., Maffei, M., Beekwilder, J., Bouwmeester, H.J., 2006. Isoprenoid biosynthesis in *Artemisia annua*: cloning and heterologous expression of a germacrene A synthase from a glandular trichome cDNA library. Arch. Biochem. Biophys. 448, 3–12.
Bork, P.M., Schmitz, M.L., Kuhnt, M., Escher, C., Heinrich, M., 1997. Sesquiterpene lactone containing Mexican Indian medicinal plants and pure sesquiterpene lactones as potent inhibitors of transcription factor NF-κB. FEBS Lett. 402, 85–90.
Bouwmeester, H.J., Kodde, J., Verstappen, F.W.A., Altug, I.G., de Kraker, J.W., Wallaart, T.E., 2002. Isolation and characterization of two germacrene A synthase cDNA clones from chicory. Plant Physiol. 129, 134–144.
Cankar, K., Houwelingen, A.v., Bosch, D., Sonke, T., Bouwmeester, H., Beekwilder, J., 2011. A chicory cytochrome P450 mono-oxygenase CYP71AV8 for the oxidation of (+)-valencene. FEBS Lett. 585, 178–182.
de Kraker, J.W., Franssen, M.C.R., Dalm, M.C.F., de Groot, A., Bouwmeester, H.J., 2001. Biosynthesis of germacrene A carboxylic acid in chicory roots. Demonstration of a cytochrome P450 (+)-germacrene A hydroxylase and NADP(+)-dependent sesquiterpenoid dehydrogenase(s) involved in sesquiterpene lactone biosynthesis. Plant Physiol. 125, 1930–1940.
de Kraker, J.W., Franssen, M.C.R., de Groot, A., Konig, W.A., Bouwmeester, H.J., 1998. (+)-Germacrene A biosynthesis - The committed step in the biosynthesis of bitter sesquiterpene lactones in chicory. Plant Physiol. 117, 1381–1392.
de Kraker, J.W., Franssen, M.C.R., Joerink, M., de Groot, A., Bouwmeester, H.J., 2002. Biosynthesis of costunolide, dihydrocostunolide, and leucodin. Demonstration of cytochrome P450-catalyzed formation of the lactone ring present in sesquiterpene lactones of chicory. Plant Physiol. 129, 257–268.
Dong, L., Miettinen, K., Goedbloed, M., Verstappen, F.W., Voster, A., Jongsma, M.A., Memelink, J., Krol, S.v.d., Bouwmeester, H.J., 2013. Characterization of two geraniol synthases from *Valeriana officinalis* and *Lippia dulcis*: similar activity but difference in subcellular localization. Metab. Eng. 20, 198–211.
Ennajdaoui, H., Vachon, G., Giacalone, C., Besse, I., Sallaud, C., Herzog, M., Tissier, A., 2010. Trichome specific expression of the tobacco (*Nicotiana sylvestris*) cembratrien-ol synthase genes is controlled by both activating and repressing cis-regions. Plant Mol. Biol. 73, 673–685.
Fischedick, J.T., Standiford, M., Johnson, D.A., De Vos, R.C.H., Todorović, S., Banjanac, T., Verpoorte, R., Johnson, J.A., 2012. Activation of antioxidant response element in mouse primary cortical cultures with sesquiterpene lactones isolated from *Tanacetum parthenium*. Planta Med. 78, 1725–1730.
Guzman, M.L., Rossi, R.M., Karnischky, L., Li, X., Peterson, D.R., Howard, D.S., Jordan, C.T., 2005. The sesquiterpene lactone parthenolide induces apoptosis of human acute myelogenous leukemia stem and progenitor cells. Blood 105, 4163–4169.

Guzman, M.L., Rossi, R.M., Neelakantan, S., Li, X.J., Corbett, C.A., Hassane, D.C., Becker, M.W., Bennett, J.M., Sullivan, E., Lachowicz, J.L., Vaughan, A., Sweeney, C.J., Matthews, W., Carroll, M., Liesveld, J.L., Crooks, P.A., Jordan, C.T., 2007. An orally bioavailable parthenolide analog selectively eradicates acute myelogenous leukemia stem and progenitor cells. Blood 110, 4427–4435.

Hagel, J.M., Yeung, E.C., Facchini, P.J., 2008. Got milk? The secret life of laticifers. Trends Plant Sci. 13, 631–639.

Heilmann, J., Wasescha, M.R., Schmidt, T.J., 2001. The influence of glutathione and cysteine levels on the cytotoxicity of helenanolide type sesquiterpene lactones against KB cells. Bioorgan. Med. Chem. 9, 2189–2194.

Houshyani, B., Assareh, M., Busquets, A., Ferrer, A., Bouwmeester, H.J., Kappers, I.F., 2013. Three-step pathway engineering results in more incidence rate and higher emission of nerolidol and improved attraction of < i > Diadegma semiclausum < /i > . Metab. Eng. 15, 88–97.

Ikezawa, N., Goepfert, J.C., Nguyen, D.T., Kim, S.-U., O'Maille, P.E., Spring, O., Ro, D.-K., 2011. Lettuce costunolide synthase (CYP71BL2) and its homolog (CYP71BL1) from sunflower catalyze distinct regio- and stereo-selective hydroxylations in sesquiterpene lactone metabolism. J. Biol. Chem. 286, 21601–21611.

Kishida, Y., Yoshikawa, H., Myoui, A., 2007. Parthenolide, a natural inhibitor of Nuclear Factor-kappaB, inhibits lung colonization of murine osteosarcoma cells. Clin. Cancer Res. 13, 59–67.

Kreuger, M.R.O., Grootjans, S., Biavatti, M.W., Vandenabeele, P., D'Herde, K., 2012. Sesquiterpene lactones as drugs with multiple targets in cancer treatment: focus on parthenolide. Anti-Cancer Drugs 23, 883–896.

Liu, Q., Majdi, M., Cankar, K., Goedbloed, M., Charnikhova, T., Verstappen, F.W.A., de Vos, R.C.H., Beekwilder, J., van der Krol, S., Bouwmeester, H.J., 2011. Reconstitution of the costunolide biosynthetic pathway in yeast and *Nicotiana benthamiana*. PLoS ONE 6, e23255.

Long, J., Ding, Y.-H., Wang, P.-P., Zhang, Q., Chen, Y., 2013. Protection-group-free semisyntheses of parthenolide and its cyclopropyl analogue. J. Org. Chem 78, 10512–10518.

Majdi, M., Liu, Q., Karimzadeh, G., Malboobi, M.A., Beekwilder, J., Cankar, K., Vos, R.d., Todorović, S., Simonović, A., Bouwmeester, H., 2011. Biosynthesis and localization of parthenolide in glandular trichomes of feverfew (*Tanacetum parthenium* L. Schulz Bip.). Phytochemistry 72, 1739–1750.

Marrs, K.A., 1996. The functions and regulation of glutathione s-transferases in plants. Annu. Rev. Plant Physiol. Plant Mol. Biol. 47, 127–158.

Mathema, V., Koh, Y.-S., Thakuri, B., Sillanpää, M., 2012. Parthenolide, a sesquiterpene lactone, expresses multiple anti-cancer and anti-inflammatory activities. Inflammation 35, 560–565.

Nasim, S., Crooks, P.A., 2008. Antileukemic activity of aminoparthenolide analogs. Bioorgan. Med. Chem. Lett. 18, 3870–3873.

Neelakantan, S., Nasim, S., Guzman, M.L., Jordan, C.T., Crooks, P.A., 2009. Aminoparthenolides as novel anti-leukemic agents: discovery of the NF-κB inhibitor, DMAPT (LC-1). Bioorgan. Med. Chem. Lett. 19, 4346–4349.

Nelson, D.R., 2009. The cytochrome P450 homepage. Hum. Genomics 4, 59–65.

Nguyen, D.T., Gopfert, J.C., Ikezawa, N., Macnevin, G., Kathiresan, M., Conrad, J., Spring, O., Ro, D.K., 2010. Biochemical conservation and evolution of germacrene A oxidase in asteraceae. J. Biol. Chem. 285, 16588–16598.

Outchkourov, N., Peters, J., De Jong, J., Rademakers, W., Jongsma, M., 2003. The promoter–terminator of chrysanthemum *rbcS1* directs very high expression levels in plants. Planta 216, 1003–1012.

Parada-Turska, J., Paduch, R., Majdan, M., Kandefer-Szerszen, M., Rzeski, W., 2007. Antiproliferative activity of parthenolide against three human cancer cell lines and human umbilical vein endothelial cells. Pharmacol. Rep. 59, 233–237.

Pareek, A., Suthar, M., Rathore, S.G., Bansal, V., 2011. Feverfew (*Tanacetum parthenium* L.): a systematic review. Pharm. Rev. 5, 103–110.

Pompon, D., Louerat, B., Bronine, A., Urban, P., 1996. Yeast expression of animal and plant P450s in optimized redox environments. Methods Enzymol. 272, 51–64.

Rodriguez, E., Towers, G.H.N., Mitchell, J.C., 1976. Biological activies of sesquiterpene lactones. Phytochemistry 15, 1573–1580.

Shanmugam, R., Jayaprakasan, V., Gokmen-Polar, Y., Kelich, S., Miller, K.D., Yip-Schneider, M., Cheng, L., Bhat-Nakshatri, P., Sledge, G.W., Nakshatri, H., Zheng, Q.H., Miller, M.A., DeGrado, T., Hutchins, G.D., Sweeney, C.J., 2006. Restoring chemotherapy and hormone therapy sensitivity by parthenolide in a xenograft hormone refractory prostate cancer model. Prostate 66, 1498–1511.

Song, J., Qian, X., Upadhyayya, P., Hong, K., Kassie, F., 2014. A water soluble parthenolide, dimethylaminoparthenolide (DMAPT), suppresses lung tumorigenesis *in vitro* and *in vivo* and downregulates the STAT3 signaling pathway. Curr. Cancer Drug Targets 14, 59–69.

Sweeney, C.J., Mehrotra, S., Sadaria, M.R., Kumar, S., Shortle, N.H., Roman, Y., Sheridan, C., Campbell, R.A., Murry, D.J., Badve, S., Nakshatri, H., 2005. The sesquiterpene lactone parthenolide in combination with docetaxel reduces metastasis and improves survival in a xenograft model of breast cancer. Mol. Cancer Ther. 4, 1004–1012.

Urban, P., Mignotte, C., Kazmaier, M., Delorme, F., Pompon, D., 1997. Cloning, yeast expression, and characterization of the coupling of two distantly related *Arabidopsis thaliana* NADPH-Cytochrome P450 reductases with P450 CYP73A5. J. Biol. Chem. 272, 19176–19186.

Vanengelen, F.A., Molthoff, J.W., Conner, A.J., Nap, J.P., Pereira, A., Stiekema, W.J., 1995. Pbinplus - an improved plant transformation vector based on Pbin19. Transgenic Res. 4, 288–290.

Wen, J., You, K.R., Lee, S.Y., Song, C.H., Kim, D.G., 2002. Oxidative stress-mediated apoptosis - The anticancer effect of the sesquiterpene lactone parthenolide. J. Biol. Chem. 277, 38954–38964.

Woods, J.R., Mo, H., Bieberich, A.A., Alavanja, T., Colby, D.A., 2011. Fluorinated amino-derivatives of the sesquiterpene lactone, parthenolide, as 19 F NMR probes in deuterium-free environments. J. Med. Chem. 54, 7934–7941.

Zhang, D.L., Qiu, L., Jin, X.Q., Guo, Z.H., Guo, C.B., 2009. Nuclear factor-κ B inhibition by parthenolide potentiates the efficacy of taxol in non-small cell lung cancer *in vitro* and *in vivo*. Mol. Cancer Res. 7, 1139–1149.

Zhang, S., Ong, C.-N., Shen, H.-M., 2004. Critical roles of intracellular thiols and calcium in parthenolide-induced apoptosis in human colorectal cancer cells. Cancer Lett. 208, 143–153.

Zhang, S., Won, Y.K., Ong, C.N., Shen, H.M., 2005. Anti-cancer potential of sesquiterpene lactones: bioactivity and molecular mechanisms. Curr. Med. Chem. 5, 239–249.